

4. Ocean-ice model (MRI.COM3)

The ocean-ice component of ESM is the MRI Community Ocean Model Version 3 (MRI.COM3). Users are referred to its reference manual (Tsujino et al., 2010) for details. Its basic characteristics are listed in Table 2. This chapter is organized as follows. Section 4.1 explains the ocean model. Section 4.2 explains the sea ice model. Section 4.3 explains how MRI.COM3 is coupled with the atmospheric component MRI-AGCM3.

Table 2: Features of MRI.COM3

Coordinates Grid arrangement (Horizontal)	General orthogonal curvilinear coordinates Arakawa B grid (coastline is on the tracer point)
Coordinates Grid arrangement (Vertical)	σ -level over z-level Partial cell at the lowermost level Bottom boundary layer (option)
Free-surface	Explicit (Killworth et al., 1991)
Momentum advection	Quasi-estrophy conservation scheme (Ishizaki and Motoi, 1999)
Sea Ice model (Thermodynamics) (Thickness category) (Dynamics)	Mellor and Kantha (1989) Hunke and Lipscomb (2006) Hunke and Dukowicz (2002)

4.1. Ocean model

4.1.1. General features

MRI.COM3 is a free-surface, depth-coordinate ocean-ice model that solves primitive equations using Boussinesq and hydrostatic approximation. A split-explicit algorithm is used for the barotropic and baroclinic parts of the equations (Killworth et al., 1991). Several upper levels follow the undulation of sea surface, as in σ -coordinate models (Hasumi, 2006). MRI.COM3 can be used to simulate ocean and sea ice with various specific configurations. Here, we describe the MRI.COM3 specification used as the ESM component. Section 4.1.2 explains resolution and topography. Section 4.1.3 explains transport algorithms for momentum and tracers. Section 4.1.4 explains sub-grid-scale mixing. Section 4.1.5 explains the solution procedure. Basic settings are summarized in Table 3.

Table 3: Settings of MRI.COM3 when used as a component of the ESM

Grid	Tripolar grid (singularities of the bipolar grid are at (64°N, 80°E) and (64°N, 100°W))
Resolution	1° (zonal), 0.5° (meridional), 50 levels + BBL (Nakano and Suginohara, 2002) (Total: 364 × 368 × 51)
Thickness of vertical grid	4, 5, 6.5, 7.5, 9, 11.5, 14, 16, 17.5, 18, 18.5, 20, 20.5, 21, 22, 23, 24, 27, 30, 30, 35, 40, 40, 50, 60, 65, 70, 75, 80, 90, 100, 100, 125, 150, 150, 150, 175, 225, 250, 250, 250, 275, 300, 300, 300, 300, 300, 450, 600, 600 (m) Upper 5 layers: variable BBL: 50 m
Tracer advection	Second-Order Moment (Prather, 1986)
Epineutral mixing (coefficients)	Isopycnal diffusion ($5 \times 10^2 \text{ m}^2\text{s}^{-1}$) + GM ¹ thickness diffusion ($2.5 \times 10^{-3} \times \text{grid-size m}^2 \text{ s}^{-1}$)
Horizontal viscosity	Smagorinsky-like viscosity with flow-dependent anisotropy
Mixed layer model	Noh and Kim (1999), Noh et al. (2005)
Background viscosity and diffusion	Tsujino et al. (2000) + Tidally driven mixing near the Kuril Islands (St. Laurent et al., 2002)

4.1.2. Resolution and topography

Horizontal resolutions are 1° of longitude and 0.5° of latitude. The model uses the Arakawa B-grid arrangement, and the coastlines are created by connecting tracer points instead of velocity points. This feature is useful for coarse-resolution global models because a narrow passage can be represented by a single velocity cell. A generalized orthogonal coordinate system is used in the Arctic region (latitudes higher than 64°N, tripolar grid; see Fig. 10).

The model ocean consists of 50 vertical levels plus a bottom boundary layer (BBL; Nakano and Suginohara, 2002). The thickness of the surface layer is 4 m, and the upper layers above 1000 m are resolved by 30 layers. The vertical levels shallower than 32 m follow the surface topography, as in σ -coordinate models (Hasumi, 2006), enabling us to obtain a fine vertical resolution near the surface without causing the uppermost layer to vanish in the southern ocean, where the sea surface height is significantly lower than in other regions. Vertically partial cells in the lowermost level enable us to

¹ Gent and McWilliams (1990)

represent realistic (smooth) bottom topography despite the rather coarse resolution of the lower layers. BBLs with a thickness of 50 m are added in dense-water formation regions.

Model topography is constructed from the Global Gridded 2-minute Database (ETOPO2v2; National Geophysical Data Center). The depth of a model grid is obtained by taking an area-weighted average of the corresponding grids in the ETOPO2v2 data. The topography of the model is modified to represent important oceanic current systems, including around complex archipelagos such as the Philippine Islands.

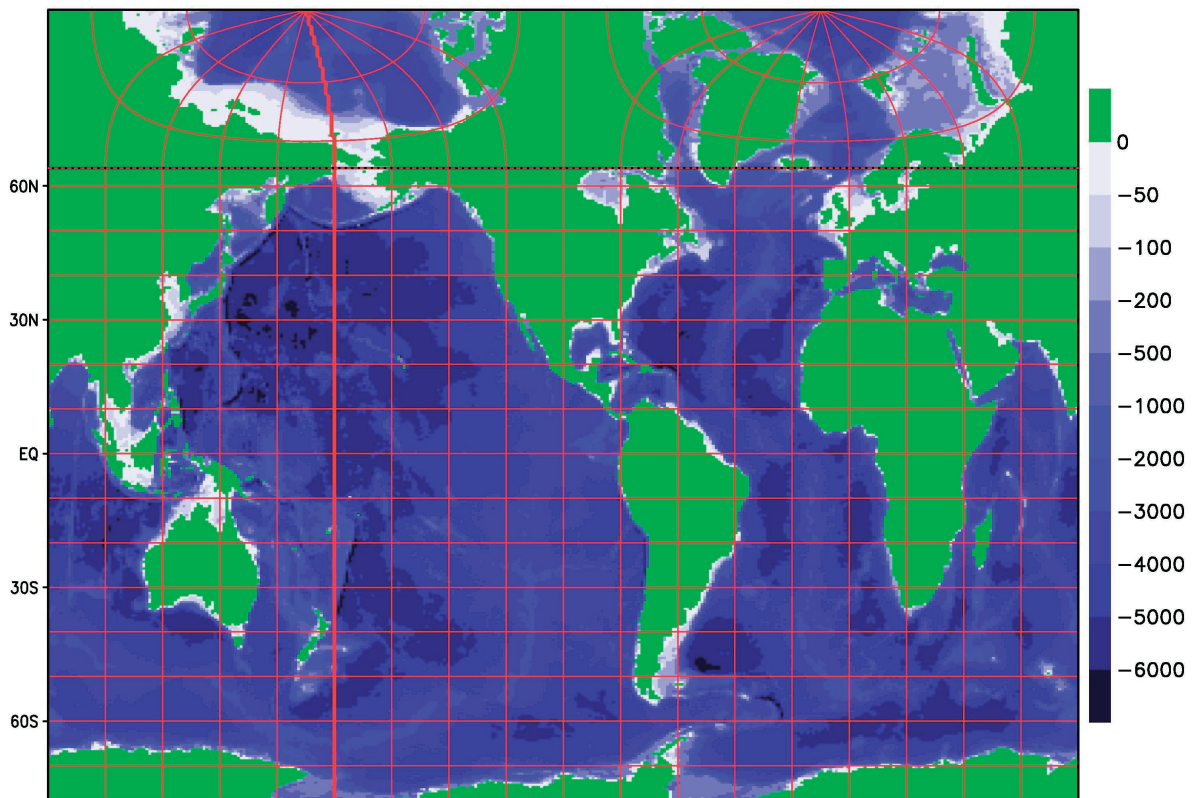


Figure 10 Topography of the ocean model component of ESM. The shades denote the bottom depth in m. The contours denote geographical latitudes and longitudes. The contour interval of latitude (longitude) is 10 (20) degree.

4.1.3. Transport algorithm

The generalized Arakawa scheme as described by Ishizaki and Motoi (1999) is used to calculate the momentum advection terms. This momentum advection scheme conserves total momentum and energy for three-dimensionally non-divergent flows over arbitrary topographies, and total quasi-entropy $((\partial v/\partial x)^2$ or $(\partial u/\partial y)^2$) for horizontally non-divergent flows.

A numerical advection scheme based on conservation of second order moments (SOM; Prather, 1986) is employed for advection of all tracers (temperature, salinity, and biogeochemical tracers). The

SOM scheme is computationally stable and almost free from numerical diffusion, so it can reproduce realistic tracer distributions in OGCMs (e.g., Hofmann and Maqueda, 2006).

4.1.4. Sub-grid-scale mixing

A flow-dependent anisotropic horizontal viscosity scheme (Smith and McWilliams, 2003) is adopted to reduce the viscosity in the direction normal to the flow (ν_N). The viscosity in the flow direction (ν_F) is set as Smagorinsky-type harmonic viscosity (Smagorinsky, 1963), $\nu_F = (4\Delta/\pi)^2 |D|$, where Δ is the grid size and $|D|$ is the strain rate. An anisotropic viscosity, $\nu_N = 0.2 \times \nu_F$, allows the equatorial undercurrent to be narrow and swift, as observed. At the lateral boundary, ν_N is set to be half of ν_F to produce a Munk boundary layer.

The following parameterizations are used for epineutral mixing processes: isopycnal diffusion (Redi, 1982; Cox, 1987) with a coefficient $500 \text{ m}^2 \text{ s}^{-1}$ and eddy-induced transport parameterized as isopycnal layer thickness diffusion (Gent and McWilliams, 1990) with a coefficient proportional to the grid size ($250 \text{ m}^2 \text{ s}^{-1}$ for 100 km).

The vertical diffusivity and viscosity are set by the turbulence closure model (Noh and Kim, 1999; Noh et al., 2005). The background vertical diffusivity consists of a horizontally uniform vertical profile, as proposed by Tsujino et al. (2000), and a parameterization for the tidally driven mixing (St. Laurent et al., 2002) near the Kuril Islands and the Sea of Okhotsk.

Seawater densities are calculated by an accurate equation of state (Tsujino et al., 2010). The vertical gravitational instabilities calculated by the model are completely eliminated at each time step by a convective adjustment scheme.

4.1.5. Solution procedure

Surface fluxes from the atmospheric component are received at the beginning of a coupling interval, and the ocean-ice component is subcycled while maintaining the global sum of the received fluxes. The relevant processes are solved in the following order.

After the local adjustments explained in section 4.3, the fluxes are used to solve the evolution of sea ice (section 4.2) and the fluxes received by the ocean are determined. Using these fluxes, the core

parts of the ocean model, the continuity equation, the baroclinic part of the momentum equation, the barotropic part of the momentum equation, and the tracer equations are solved in the order listed. The evolved states are checked for static stability, and the turbulence closure model is solved to determine vertical mixing coefficients for the next time step.

Snapshots of surface properties are sent to the atmospheric component at the end of each coupling interval.

Basically, a leap-frog scheme is employed for a time-integration. By default, the Matsuno (Euler-backward) scheme is used once per 12 time steps to suppress computational noise. This interval can be changed at run time by using a namelist parameter. A common time step is used for all processes except for the barotropic part of the momentum equation (the time step of which is independently specified). Starting at the same time as the baroclinic part, the barotropic part is subcycled (by the split-explicit method) and integrated for two baroclinic time steps. The average state during these two baroclinic time steps is returned. Typically, the time step of the ocean-ice component is 30 minutes and that of the barotropic part is 1 minute.

4.2. Sea ice model

4.2.1. General features

The sea ice part solves the fractional area, heat content, thickness, and the transport of ice categorized according to its thickness and the dynamics of the grid-cell-averaged ice pack. Heat, water, salt, and momentum fluxes are exchanged with the atmosphere and ocean. Using Scup, the sea ice part sends surface temperature, interior temperature, snow and ice thicknesses, and fractional area to the atmospheric component, and receives surface fluxes calculated by that component. The ice model is part of the ocean model and ice–ocean exchange processes are internal.

The thermodynamic part is based on Mellor and Kantha (1989). For processes that are neither explicitly discussed nor included by Mellor and Kantha (1989), such as categorization by thickness, ridging, and rheology, we adopt those of the Los Alamos sea ice model (CICE; Hunke and Lipscomb, 2006). The formulation and solving procedure of each process are briefly presented in later sections. See the MRI.COM reference manual (Tsujino et al., 2010) for details.

The fundamental property that defines the state of sea ice is its fractional area as a function of location (x, y) and thickness (h) . The equation for this distribution function, $g(x, y, h)$, is expressed as follows:

$$\frac{\partial g}{\partial t} = \frac{\partial}{\partial h} (fg) - \frac{1}{h_\mu h_\psi} \left(\frac{\partial (gh_\psi u_I)}{\partial \mu} + \frac{\partial (gh_\mu v_I)}{\partial \psi} \right) - \chi \quad (4.1)$$

where f is the thermodynamic growth rate of ice thickness, (u_I, v_I) is the velocity vector of an ice pack, and χ is the rate of change of the distribution function caused by mechanical ridging. We discretize the thickness into five categories, separated at $H_n = 0.0, 0.6, 1.4, 2.4, 3.6,$ and 30.0 m. The fractional area of the n -th category (a_n) is defined as follows:

$$a_n = \int_{H_{n-1}}^{H_n} g dh \quad (4.2)$$

Other major variables, ice and snow thickness, surface temperature, bottom temperature and salinity, and internal energy of ice, are defined for each category. Velocity is defined for an ice pack, the total ice mass in a grid cell. In the vertical direction, both ice and snow have one layer; the heat capacity of sea ice, but not of snow, is considered. The heat capacity of sea ice is due to brine and is represented by the temperature at the center of the ice. It is assumed that sea ice has the same energy (temperature) throughout the layer.

The growth rate of ice thickness is computed by solving thermodynamic processes (Section 4.2.2). Using this growth rate (f), thickness categories are remapped according to the first term on the right-hand side (r.h.s.) of Eq. (4.1) (Section 4.2.3). To compute the velocity of an ice pack (u_I, v_I) , we have to solve the momentum equation (Section 4.2.4). When the ice distribution is transported (second and third terms on the r.h.s. of Eq. (4.1)), other conservative properties such as volume and energy are also transported (Section 4.2.5). The ridging process (χ ; fourth term on the r.h.s. of Eq. (4.1)) is solved with the transported ice distribution function (Section 4.2.6).

4.2.2. Thermodynamics

In considering the thermodynamics, the thermal energy of sea ice should be defined. The energy base (i.e., zero energy) is defined here as that of seawater at 0°C . The thermal energy (enthalpy; $E(T, r)$)

of sea ice with temperature T_1 (<0 °C) and brine (salt water) fraction r is the negative of the energy needed to raise the temperature of the ice to 0 °C and melt all of it:

$$E(T, r) = r(C_{po}T) + (1-r)(-L_F + C_{pi}T) \quad (4.3)$$

where C_{po} and C_{pi} are the specific heats of seawater and sea ice, respectively, and L_F is the latent heat of melting/freezing. The brine fraction of sea ice is $r = S_I / S = mS_I/T_1$, where S_I (= 4.0 practical salinity units; psu) is the salinity of ice, T_1 is the temperature of ice defined at its center, and m determines the freezing temperature as a function of salinity.

Heat fluxes relevant to thermodynamic processes are surface heat fluxes from the atmosphere (short- and longwave radiations, latent and sensible heat fluxes), heat conduction within ice and snow, and heat fluxes between the ice bottom and the first ocean layer.

Operations to solve sea ice thermodynamic processes proceed as follows.

If the temperature of the first layer of the ocean model is below the freezing point as a function of salinity, the temperature is set to the freezing point, and the heat needed to raise the temperature, regarded as the release of latent heat, is used to form new and frazil ice. For a grid cell without sea ice, the initial ice thickness is set to 0.1 m and the fractional area is determined from the ice volume. For a grid cell where sea ice already exists, the grid mean thickness is added to each category and to open water.

The surface temperature at the top surface is computed so that the fluxes on both sides, the atmospheric heat flux and the ice interior flux, are the same. A semi-implicit method is adopted. If a new surface temperature is below the freezing point, melting does not occur. If it is not, the surface temperature is set to the freezing temperature (mS_I), and the heat flux in the ice interior is re-evaluated. The amount of melting is obtained from the imbalance.

In the ice interior, thermal energy changes according to the vertical heat flux budgets in the upper and lower parts of the ice.

At the bottom, the balances of the heat and salt fluxes, which involve the heat flux in the ice interior, fluxes caused by freezing or melting at the interface, and fluxes caused by molecular diffusion in the surface skin layer, are imposed and solved simultaneously. The same operation is applied to the open water using the air–sea flux (without solar radiation) and the surface skin layer flux.

Solar radiation in the infrared band is absorbed at the top surface. A fraction of radiation in the visible band penetrates into the ice layer and attenuates with an e -folding scale of 1.4 m^{-1} , warming the ice interior. The remainder penetrates into the ocean.

4.2.3. Vertical remapping

After the thermodynamic processes are solved, the resultant ice thickness in some thickness categories might not be within the specified bounds. Following the same method as that used in CICE, we assume that there is a thickness distribution function in each category and use it to redistribute the new thickness distribution into the original categories. Specifically, a thickness category is regarded as a Lagrange particle, and the category boundaries are displaced as a result of thermodynamics. The growth and melting rate in each category is linearly interpolated to obtain a the displacement speed of the category boundary. A linear thickness distribution function is assumed within each displaced category, and ice is remapped into the original categories by using these functions.

4.2.4. Dynamics

The equation of motion used for an ice pack is that for a continuous medium, as follows:

$$\rho_I \frac{\partial(Ah_I u_I)}{\partial t} - \rho_I Ah_I f v_I = -\rho_I Ah_I g \frac{1}{h_\mu} \frac{\partial h}{\partial \mu} + F_\mu(\sigma) + A(\tau_{AI\mu} + \tau_{IO\mu}) \quad (4.4)$$

$$\rho_I \frac{\partial(Ah_I v_I)}{\partial t} + \rho_I Ah_I f u_I = -\rho_I Ah_I g \frac{1}{h_\psi} \frac{\partial h}{\partial \psi} + F_\psi(\sigma) + A(\tau_{AI\psi} + \tau_{IO\psi}) \quad (4.5)$$

where A is concentration, h_I is thickness, and ρ_I is density of an ice pack. An ice pack is forced by stress from wind at the top (τ_{AI}) and stress from oceanic currents at the bottom (τ_{IO}). The motion is also affected by the Coriolis force (the terms with the Coriolis parameter f), the sea-level slope (h), and the internal stress of the ice ($F(\sigma)$).

To estimate the internal stress, the elastic-plastic-viscous (EVP) model by Hunke and Dukowicz (2002) is adopted as the constitutive law (the relation between stress and strain rate). The EVP model is a computationally efficient modification of the viscous-plastic model (Hibler, 1979). The EVP model treats the ice as an elastic medium, and a large local force is released by elastic waves, which would be

damped within the timescale of the wind forcing. The dynamics scheme is subcycled within the thermodynamic time step.

4.2.5. Transport

Fractional area, snow volume, ice volume, ice energy, and ice surface temperature of each category are transported using the drifting velocity of the ice pack. A multidimensional positive definite advection transport algorithm (MPDATA; Smolarkiewicz, 1984) is used. The MPDATA scheme is suitable for the transport of ice because all transported properties should be sign-definite in the ice model.

4.2.6. Ridging and adjustment

As a result of advection, the sum of the fractional areas of a grid cell might exceed one, especially where the velocity field is convergent. In such a case, it is assumed that ridging occurs in the ice to yield a sum equal to or less than one. Even if the sum is less than one, ridging or rafting might occur where the concentration of ice is high. The ridging rate is a function of deformation rates. The ridging scheme of MRI.COM3 follows that of CICE, as detailed in the MRI.COM3 reference manual.

Finally, the part of snow that is below freeboard in accordance with Archimedes' principle absorbs seawater to become sea ice. The appropriate amount of salt is extracted from the ocean.

4.2.7. Solution procedure

The sea ice model is called from the ocean model once during each oceanic time step. Thus, the time step of the processes except for the dynamics (momentum equation) is the same as that of the ocean model. The momentum equation is subcycled. Typically, the time step for the thermodynamics is 30 minutes and that for the momentum equation is 1 minute (the time steps can be specified by the user at run time).

The sea ice model uses the forward scheme of time integration and is not called from the ocean model in the backward phase of the Matsuno (Euler-backward) scheme. The momentum equation uses the backward scheme.

All variables except for ice pack velocity and stresses are defined at the tracer point of Arakawa's B-grid arrangement. Spatial discretization for transport and momentum equations uses the centered difference.

4.3. Exchange of properties with the atmospheric component

The exchange of properties with the MRI-AGCM3 atmospheric component is realized by using the simple Scup coupler developed by Yoshimura and Yukimoto (2008). The coordinate transformation tables in both exchange directions should be prepared prior to integration. The coupling interval can be specified by the user at run time. It should be a common multiple of the time steps in the atmosphere and ocean components. It is normally set to 1 hour. The time step for the ocean model is normally 30 minutes.

The boundary between MRI-AGCM3 and MRI.COM3 is placed at the bottom of the atmosphere. The fluxes above the boundary are computed by MRI-AGCM3 and received by MRI.COM3 at the beginning of a coupling interval (section 4.3.1). Sea-surface properties are sent to MRI-AGCM3 at the end of a coupling interval (section 4.3.2).

4.3.1. From atmosphere to ocean

Surface fluxes are calculated in MRI-AGCM3 and accumulated during a coupling interval. The mean fluxes during this interval are then sent to MRI.COM3. Thus, MRI.COM3 uses the surface fluxes averaged over the last 1 hour. These fluxes are kept unchanged during a coupling interval.

The following properties are exchanged.

Grid cell mean:

- Precipitation
- Sea-level pressure
- Scalar wind speed above seawater at 10 m height
- Surface wind stress on seawater
- Scalar wind stress (friction velocity) on seawater
- Scalar wind speed above sea ice at 10 m height

- Surface wind stress on sea ice
- Scalar wind stress (friction velocity) on sea ice
- Water flux due to river discharge
- Heat flux due to river discharge
- Water flux due to iceberg discharge
- Heat flux due to iceberg discharge

Separated into open-water and ice-thickness categories:

- Net long-wave radiation (upward + downward)
- Latent heat flux
- Sensible heat flux
- Net shortwave radiation (direct and visible)
- Net shortwave radiation (diffuse and visible)
- Net shortwave radiation (direct and near infrared)
- Net shortwave radiation (diffuse and near infrared)
- Evaporation/condensation/sublimation
- Surface skin temperature
- CO₂ flux at the sea surface

4.3.2. From ocean to atmosphere

The following properties (snapshots) are sent to MRI-AGCM3 at the end of a coupling interval.

- Temperature in the first level
- Salinity in the first level
- Velocity vector in the first level
- Fractional area of ice pack (all categories)
- Ice thickness (all categories)
- Snow thickness (all categories)
- Temperature at the ice or snow surface (all categories)
- Interior temperature of ice (all categories)
- Oceanic pCO₂

4.3.3. Use of surface fluxes and adjustment for conservation

The atmospheric component evaluates surface fluxes, and the ocean-ice MRI.COM3 component uses these fluxes to solve the evolution of sea-surface states and the growth and melting of sea ice.

The surface fluxes are kept basically unchanged in MRI.COM3 during a coupling interval. The following three-step procedure is used to ensure conservation. First, a numerical error that could arise during coordinate transformation is adjusted: Globally averaged total fluxes of heat and freshwater are evaluated before and after the transformation. The difference in the globally averaged heat fluxes is added to the total long-wave flux and that in the freshwater fluxes is added to precipitation or evaporation, depending on the sign of the difference.

Second, the evolution of the sea ice area during a coupling interval is considered because it would immediately result in changes to the globally averaged fluxes. These changes are evaluated at each time step, and global flux adjustments are imposed on the heat flux and freshwater flux as in the first step.

Finally, the evolution of ice surface temperature is considered. Without a feedback mechanism (i.e., with fluxes fixed), the ice surface skin temperature obtained by imposing the flux balance would exhibit unstable behavior. To prevent this, the ice surface skin temperature used for evaluating upward blackbody radiation is updated at each time step of MRI.COM3 during a coupling interval. The resultant inconsistencies in total longwave fluxes are averaged globally and added to the heat flux between ice and ocean. Thus, the residual flux is consumed by the ocean. Note that the sum of heat flux adjustments arising from these procedures is typically less than 1 W m^{-2} .